ORIGINAL ARTICLE

Hydrodynamic Turbulence: Sweeping Effect and Taylor's Hypothesis via Correlation Function

Mahendra K. Verma[1] · Abhishek Kumar[2] · Akanksha Gupta[1]

Abstract

We demonstrate the sweeping effect in turbulence using numerical simulations of hydrodynamic turbulence without a mean velocity. The velocity correlation function, $C(\mathbf{k}, \tau)$, decays with time due to the eddy viscosity. In addition, $C(\mathbf{k}, \tau)$ shows oscillations due to the sweeping effect by "random mean velocity field" $\tilde{\mathbf{U}}_0$. We also perform numerical simulation with mean velocity $\mathbf{U}_0 = 10\hat{z}$ (10 times the rms speed) for which $C(\mathbf{k}, \tau)$ exhibits damped oscillations with the frequency of $|\mathbf{U}_0|k$ and decay time scale corresponding to the $\mathbf{U}_0 = 0$ case. For $\mathbf{U}_0 = 10\hat{z}$, the phase of $C(\mathbf{k}, \tau)$ shows the sweeping effect, but it is overshadowed by oscillations caused by $\mathbf{U}_0$. We also demonstrate that for $\mathbf{U}_0 = 0$ and $10\hat{z}$, the frequency spectra of the velocity fields measured by real-space probes are respectively f^{-2} and $f^{-5/3}$; these spectra are related to the Lagrangian and Eulerian space-time correlations respectively.

Keywords Turbulence · Sweeping effect · Taylor's hypothesis · Hydrodynamic turbulence

Introduction

The incompressible Navier–Stokes equations of a flow that is moving with a mean velocity of $\mathbf{U}_0$ is

$$\frac{\partial \mathbf{u}}{\partial t} + (\mathbf{u} \cdot \nabla)\mathbf{u} + (\mathbf{U}_0 \cdot \nabla)\mathbf{u} = -\nabla p + \nu \nabla^2 \mathbf{u} + \mathbf{f}, \tag{1}$$

$$\nabla \cdot \mathbf{u} = 0, \tag{2}$$

where $\mathbf{u}$ is the velocity fluctuation with a zero mean, $\mathbf{f}$ is the external force, p is the pressure, and ν is the kinematic viscosity. One of the important principles of classical physics is Galilean invariance, according to which the laws of physics are the same in all inertial frames (frames moving with constant velocities relative to each other). Naturally, the Navier–Stokes equations, which are essentially Newton's laws for fluid flows, exhibits this symmetry (Lesieur 2012; Frisch 1995; Davidson 2015; McComb 1990, 2014; Belinicher and L'vov 1987). As a consequence of this symmetry,

the flow properties of the fluid in the laboratory reference frame (in which the fluid moves with a mean velocity of $\mathbf{U}_0$) and in the co-moving reference frame ($\mathbf{U}_0 = 0$) are the same.

The velocity field of a turbulent flow is random; hence it is typically characterised by its correlations. There have been several major advances in the understanding the correlations in homogeneous and isotropic turbulence, most notably by Kolmogorov (1941a, b) who showed that in the inertial range, the velocity correlation $C(\mathbf{k}) = \langle |\mathbf{u}(\mathbf{k})|^2 \rangle = K_{\mathrm{Ko}} \epsilon^{2/3} k^{-5/3}/(4\pi k^2)$, where ϵ is the energy dissipation rate, and K_{Ko} is the Kolmogorov constant. The corresponding one-dimensional energy spectrum is $E(k) = K_{\mathrm{Ko}} \epsilon^{2/3} k^{-5/3}$. Note that ϵ equals the energy flux in the inertial range.

Kraichnan (1964) argued that in the presence of a "random mean velocity" field, $\tilde{\mathbf{U}}_0$, Eulerian field theory does not yield Kolmogorov's spectrum. In particular, Kraichnan (1964) considered a fluid flow with $\tilde{\mathbf{U}}_0$ that is constant in space and time but has a Gaussian and isotropic distribution over an ensemble of realisations. Then he employed direct interaction approximation (DIA) to close the hierarchy of equations and showed that $E(k) \sim (\epsilon \tilde{U}_0)^{1/2} k^{-3/2}$, where $\tilde{U}_0$ is the root mean square (rms) value of the mean velocity. Kraichnan (1964) argued that the above deviation of the energy spectrum from the experimentally observed Kolmogorov's $k^{-5/3}$ energy spectrum is due to the sweeping of small-scale fluid structures by

✉ Mahendra K. Verma
mkv@iitk.ac.in

1 Department of Physics, Indian Institute of Technology Kanpur, Kanpur 208016, India

2 Centre for Fluid and Complex Systems, Coventry University, Coventry CV1 5FB, UK

the large energy-containing eddies. This phenomenon is called sweeping effect. Based on the above observations, Kraichnan (1964) emphasised that the Eulerian formalism is inadequate for obtaining Kolmogorov's spectrum for a fully developed fluid turbulence. Later, he developed Lagrangian field theory for hydrodynamic turbulence that is consistent with the Kolmogorov's 5/3 theory of turbulence (see Kraichnan 1965, and other related papers). The above framework is called random Galilean invariance (Kraichnan 1964).

There have been several attempts to test the sweeping effect. Kraichnan (1964) had argued that the nonlinear time scale is $1/(k\tilde{U}_0)$ due to the dependence on the mean random velocity $\tilde{U}_0$, and hence the energy spectrum $E(k) \sim (\epsilon \tilde{U}_0)^{1/2} k^{-3/2}$. Sanada and Shanmugasundaram (1992) computed the time scale for the decay of the correlation function for various k's, and argued it to vary as k^{-1}, in line with the predictions of Kraichnan (1964). Based on these results, Sanada and Shanmugasundaram (1992) argued that their correlation function validates the sweeping effect. In a related work, Drivas et al. (2017) employed spatial filtering to study the sweeping effect on small-scale velocities by a large-scale flow. They showed consistency between results of direct numerical simulation and large-eddy simulation with appropriate filtering.

He et al. (2010) and He and Tong (2011) proposed elliptic model in which the isocorrelation lines of two-point two-time velocity correlations are ellipses parameterised by the mean and sweeping velocities. Note that the mean velocity $\mathbf{U}_0$ is related to the Taylor's frozen-in hypothesis (to be described below). Researchers observed that the elliptic model describes several experimental and direct numerical simulation (DNS) data more accurately than the classic Taylor's hypothesis. Thus, the elliptic model validates the sweeping effect in hydrodynamic turbulence. Wilczek and Narita (2012) derived the frequency spectrum of hydrodynamic turbulence based on sweeping effect and mean flow. Their results are consistent with the sweeping effect and elliptic model.

A related phenomenon is Taylor's hypothesis of frozen-in turbulence. Taylor (1938) proposed that the velocity measurement at a point in a fully-developed turbulent flow moving with a constant velocity $\mathbf{U}_0$ (e.g. in a wind tunnel) can be used to study the velocity correlations. Taylor's hypothesis works because the mean flow advects the frozen-in fluctuations, and the stationary probe in the fluid measures the fluctuations along a line. Here, the frequency spectrum of the measured time series is expected to show $f^{-5/3}$, where f is the frequency. Taylor's frozen-in turbulence hypothesis has been used in many experiments to ascertain Kolmogorov's spectrum (Tennekes and Lumley 1972). As discussed above, Taylor's frozen-in hypothesis is incorporated in the elliptic model (He et al. 2010; He and Tong 2011) and in Wilczek and Narita model (Wilczek and Narita 2012).

In this paper, our approach is somewhat different from the earlier ones. We compute the normalised correlation function

for the velocity Fourier mode and find this to be complex, unlike Sanada and Shanmugasundaram (1992)'s function which is real. The phase of the correlation function helps us deduce the random mean velocity that is responsible for the sweeping effect. We thus provide definitive evidence for the sweeping effect. In addition, we also analyse the correlation function with and without a mean velocity, as well as the frequency spectrum. In Section "Taylor's Frozen-in hypothesis for $\mathbf{U}_0 \neq 0$, and frequency spectrum" we show that the frequency spectrum $E(f) \sim f^{-2}$ for turbulent flow in the absence of a constant mean velocity field $\mathbf{U}_0$, and $E(f) \sim f^{-5/3}$ for large U_0.

In the next two sections, we briefly describe the Green's functions, correlation function, and sweeping effect in hydrodynamic turbulence. In Sections "New evidences for the sweeping effect" and "Sweeping effect for $\mathbf{U}_0 \neq 0$" we demonstrate the signatures of sweeping effect using numerical simulations with and without mean velocity. In Section "Taylor's Frozen-in hypothesis for $\mathbf{U}_0 \neq 0$, and frequency spectrum" we revisit Taylor's hypothesis in light of sweeping effect. We conclude in Section "Discussions and conclusions".

A Brief Review of Green's Function and Correlation Function in Hydrodynamic Turbulence

Kraichnan (1964) derived the sweeping effect using direct interaction approximation (DIA) (Kraichnan 1959). We will sketch sweeping effect in the next section. However its description requires some terminologies, such as Green's function, correlation function, and effective viscosity, which will be briefly described below. See Kraichnan (1959) and Leslie (1973) for details.

A linearised version of Eq. (1) in Fourier space is

$$\left(\frac{\partial}{\partial t} + i\mathbf{U}_0 \cdot \mathbf{k} + \nu k^2\right)\mathbf{u}(\mathbf{k}) = \mathbf{f}(\mathbf{k}), \tag{3}$$

where $\mathbf{k}$ is the wavevector. The corresponding equation for the Green's function is

$$\left(\frac{\partial}{\partial t} + i\mathbf{U}_0 \cdot \mathbf{k} + \nu k^2\right)G(\mathbf{k}, t, t') = \delta(t - t'), \tag{4}$$

whose solution is

$$G(\mathbf{k}, \tau) = \theta(\tau) \exp\left(-i\mathbf{U}_0 \cdot \mathbf{k} t\right) \exp\left(-\nu k^2 \tau\right), \tag{5}$$

where $\tau = t - t'$, and $\theta(\tau)$ is the step function.

In addition, the equal-time correction function, $C(\mathbf{k}, 0)$, and unequal time correction function, $C(\mathbf{k}, \tau)$, for the velocity mode with wavenumber $\mathbf{k}$ are defined as

$$C(\mathbf{k}, 0) = \langle |\mathbf{u}(\mathbf{k}, t)|^2 \rangle, \tag{6}$$

$$C(\mathbf{k}, \tau) = \langle \mathbf{u}(\mathbf{k}, t) \cdot \mathbf{u}^*(\mathbf{k}, t + \tau) \rangle. \tag{7}$$

In the above, the averaging could be either ensemble or temporal (due to homogeneity in time). The ratio of the two correlation function is the normalised correlation function:

$$R(\mathbf{k}, \tau) = \frac{C(\mathbf{k}, \tau)}{C(\mathbf{k}, 0)}. \tag{8}$$

A generalisation of fluctuation–dissipation theorem to hydrodynamics yields (Kiyani and McComb 2004)

$$R(\mathbf{k}, \tau) = G(\mathbf{k}, \tau) = \theta(\tau) \exp(-i\mathbf{U}_0 \cdot \mathbf{k}t) \exp(-\nu k^2 \tau). \tag{9}$$

That is, the normalised correlation function exhibits damped oscillations—oscillations due to $\mathbf{U}_0$, while damping arising from the viscous part.

Researchers attempted to incorporate the effects of nonlinearity in the above functions. The methods used are DIA (Kraichnan 1959; Leslie 1973), Lagrangian field theory (Kraichnan 1965), renormalisation groups (Yakhot and Orszag 1986; McComb 1990; De Dominicis and Martin 1979; Zhou 2010), etc. We do not detail these methods here, but we state several important results derived using these computations:

1. Using field theory and certain assumptions, researchers have been able to show that the nonlinearity yields enhanced viscosity at a wavenumber k in the following manner:

    $$\nu \to \nu + \nu(k), \tag{10}$$

    where $\nu(k)$, called "effective viscosity" or "renormalized viscosity", is

    $$\nu(k) = \nu_* \sqrt{K_{\mathrm{Ko}}} \epsilon^{1/3} k^{-4/3}, \tag{11}$$

    with ν_* as a constant. Physically, $\nu(k)$ represents the effective viscosity at wavenumber k. For large k's (in the inertial range), $\nu(k) \gg \nu$, hence the total viscosity is essentially $\nu(k)$. This viscosity leads to enhanced mixing. In other words, the effective Navier-Stokes equation in the presence of nonlinearity is

    $$\left(\frac{\partial}{\partial t} + i\mathbf{U}_0 \cdot \mathbf{k} + [\nu + \nu(k)]k^2\right)\mathbf{u}(\mathbf{k}) = \mathbf{N}(\mathbf{k}) + \mathbf{f}(\mathbf{k}), \tag{12}$$

    where $\mathbf{N}(\mathbf{k})$ is the nonlinear term (including the pressure gradient). Refer to Yakhot and Orszag (1986), McComb (1990), De Dominicis and Martin (1979) and Zhou (2010)) for details. Also see "Appendix 1: Sweeping effect and renormalization in Eulerian framework".

2. Using Eq. (12) and certain assumptions on the perturbation, Green's function of Eq. (5) gets transformed to the following form for the Navier-Stokes equations with the nonlinear terms:

$$
\begin{aligned}
G(\mathbf{k}, \tau) &= \theta(\tau) \exp(-i\mathbf{U}_0 \cdot \mathbf{k}t) \exp(-\nu(k)k^2 \tau) \\
&= \theta(\tau) \exp(-i\mathbf{U}_0 \cdot \mathbf{k}t) \exp(-\tau/\tau_c),
\end{aligned} \tag{13}
$$

where

$$\tau_c = \frac{1}{\nu(k)k^2} \sim \frac{1}{\epsilon^{1/3} k^{2/3}}. \tag{14}$$

is the decay time scale. Since $\nu(k) \gg \nu$, the decay time scale for Eq. (13) is much smaller than the corresponding time scale for Eq. (5). The above Green's function is called "dressed Green's function" in field theory.

3. For the nonlinear equation, using field-theoretic treatment and generalisation of fluctuation-dissipation theorem, the correlation function of Eq. (9) is generalised to

$$R(\mathbf{k}, \tau) = G(\mathbf{k}, \tau) = \theta(\tau) \exp(-i\mathbf{U}_0 \cdot \mathbf{k}t) \exp(-\nu(k)k^2 \tau). \tag{15}$$

    That is, the decay time scale for the correlation function is same as that for the Green's function.

4. In the absence of $\mathbf{U}_0$, the correlation and Green's functions are:

$$R(\mathbf{k}, \tau) = G(\mathbf{k}, \tau) = \theta(\tau) \exp(-\nu(k)k^2 \tau). \tag{16}$$

    The above function exhibits pure damping.

In the following section we provide a brief introduction to the sweeping effect.

Brief Description of Sweeping Effect

In this section, we briefly describe the sweeping effect (Kraichnan 1964). Kraichnan assumed that the velocity fluctuations of Navier–Stokes equations is advected by random large-scale flow, $\tilde{\mathbf{U}}_0$. Note the contrast in notation between the random large-scale flow, $\tilde{\mathbf{U}}_0$, and the mean velocity, $\mathbf{U}_0$. Kraichnan (1964) ignored the viscous and nonlinear terms, and simplified Eq. (12) to

$$\left(\frac{\partial}{\partial t} + i\tilde{\mathbf{U}}_0 \cdot \mathbf{k}\right)\mathbf{u}(\mathbf{k}) = \mathbf{f}(\mathbf{k}). \tag{17}$$

For the above equation, the normalized correlation function is obtained by setting $\nu = 0$ in Eq. (9):

$$R(\mathbf{k}, \tau) = \theta(\tau) \exp(-i\tilde{\mathbf{U}}_0 \cdot \mathbf{k}t). \tag{18}$$

Kraichnan (1964) further assumed that $\tilde{\mathbf{U}}_0$ is constant in time, but it is spatially varying with a Gaussian distribution. We could consider $\tilde{\mathbf{U}}_0$ to be of the order of rms (root mean square) speed. Under these assumptions, the averaged correlation function has the following form (also see Wilczek and Narita 2012):

$$R(\mathbf{k}, \tau) = \langle \exp[-i\mathbf{k} \cdot \tilde{\mathbf{U}}_0 \tau] \rangle = \exp\left[-\frac{\langle \tilde{U}_0^2 \rangle k^2 \tau^2}{6} \right]. \qquad (19)$$

Note that the above averaging with Gaussian $\tilde{U}_0$ differs from the ensemble or temporal averaging performed for the correlation function of Eq. (7).

Using the above equation and field-theoretic arguments, Kraichnan (1964) argued that the relevant nonlinear time scale is $1/(k\tilde{U}_0)$ that would yield the following energy spectrum:

$$E(k) \sim (\epsilon \tilde{U}_0)^{1/2} k^{-3/2}, \qquad (20)$$

where ϵ is the energy dissipation rate. The above spectrum is very different from Kolmogorov's prediction that $E(k) \sim \epsilon^{2/3} k^{-5/3}$, which is observed in experiments. Based on these contradictions, Kraichnan (1964) argued that Eulerian field theory is inadequate to reproduce $k^{-5/3}$ energy spectrum, and hence unsuitable for describing turbulence. He went on to develop Lagrangian field theory to reproduce the consistent energy spectrum (Kraichnan 1965).

In this paper we test the sweeping effect using numerical simulation. Note that due random nature of large-scale flow $\tilde{\mathbf{U}}_0$,

$$\begin{aligned} R(\mathbf{k}, \tau) &= \exp(-\tau/\tau_c(k)) \exp(-i\tilde{\mathbf{U}}_0 \cdot \mathbf{k}\tau) \\ &\rightarrow \exp(-\tau/\tau_c(k)) \exp(-ick\tilde{U}_0\tau), \end{aligned} \qquad (21)$$

where c is a random number that can take both positive and negative values. In the present paper we compute $R(\mathbf{k}, \tau)$ and look for a signature of random $\tilde{U}_0$ in the phase of $R(\mathbf{k}, \tau)$. A nonzero phase in Eq. (21) would signal a presence of $\tilde{\mathbf{U}}_0$, hence the sweeping effect. Note that our proposed correlation function of Eq. (22) differs from Eq. (19) of Kraichnan (1964). We do not make any assumption on the probability distribution of $\tilde{\mathbf{U}}_0$. This process helps us examine oscillations in $R(\mathbf{k}, \tau)$ induced by $\tilde{\mathbf{U}}_0$.

In the presence of a mean velocity field $\mathbf{U}_0$, the correlation function of Eq. (15) with sweeping effect is expected to be of the following form:

$$\begin{aligned} R(\mathbf{k}, \tau) &= \exp(-\tau/\tau_c(k)) \exp(-i\mathbf{U}_0 \cdot \mathbf{k}\tau - i\tilde{\mathbf{U}}_0 \cdot \mathbf{k}\tau) \\ &\rightarrow \exp(-\tau/\tau_c(k)) \exp(-ick\tilde{U}_0\tau) \exp(-i\mathbf{U}_0 \cdot \mathbf{k}\tau). \end{aligned} \qquad (22)$$

The above correlation function includes sweeping effect along with oscillations arising due to $\mathbf{U}_0$. The Fourier transfer of the above equation to the frequency space yields the following Green's function in $(\mathbf{k}, \omega)$ space:

$$G(\mathbf{k}, \omega) = \frac{1}{-i\omega + \nu(k)k^2 + i\mathbf{U}_0 \cdot \mathbf{k} + ick\tilde{U}_0(k)}. \qquad (23)$$

In the next section we provide numerical evidences for the sweeping effect.

New Evidences for the Sweeping Effect

In this section, we demonstrate the existence of wavenumber dependent phases of $R(\mathbf{k}, \tau)$, thus signalling the presence of sweeping effect. We perform a numerical simulation of Navier–Stokes equations in the turbulent regime for the mean velocity $\mathbf{U}_0 = 0$. We employ pseudospectral code TARANG (Verma et al. 2013; Chatterjee et al. 2017) to simulate the flow on 512^3 and 1024^3 grids with random forcing (Novikov 1965). For the forcing, we employ the procedure proposed by Carati et al. (1995). We use the fourth-order Runge Kutta (RK4) scheme for time stepping, 2/3 rule for dealiasing, and CFL condition for computing Δt.

In our manuscript, we adopt nondimensional units for all the relevant quantities. As is customary, we nondimensionalize length and velocity using systems size and velocity (here, rms speed, u_{rms}) respectively. Hence, in our simulation, the rms speed is approximately unity, and the mean velocity ($\mathbf{U}_0$) is the velocity relative to the rms speed. For the present set of simulations, we use $L = 2\pi$, and the unit of time as eddy turnover time, L/u_{rms}. The parameters of our simulations are described in Table 1. The Reynolds number of the runs are $u_{rms}L/\nu = 5.7 \times 10^3$ for 512^3 grid, and 1.3×10^4 for 1024^3 grid. All our simulations are fully resolved since $k_{max}\eta > 1$, where k_{max} is the maximum wavenumber of the run, and η is the Kolmogorov length scale.

We evolve the flow with $\mathbf{U}_0 = 0$ till a steady state is reached. At this point, we fork the above run to two new simulations with $\mathbf{U}_0 = 0$ and $\mathbf{U}_0 = 10\hat{z}$. The new runs are carried out up to one eddy turnover time each. For $\mathbf{U}_0 = 0$ and $\mathbf{U}_0 = 10\hat{z}$, the temporal evolution of the fluctuating energy and the energy spectra are identical, as illustrated in Fig. 1; this is consistent with the Galilean invariance of the Navier–Stokes equations. These results, however, are based on equal-time correlations; subtleties, however, emerge when we study the temporal correlations of the velocity Fourier modes.

Using the steady state numerical data of 1024^3 grid, we compute the normalised correlation function $R(\mathbf{k}, \tau)$ of Eq. (8) for $k = 10, 12, 15, 20,$ and 22 that lie in the inertial range. The correlation $R(\mathbf{k}, \tau)$ was time averaged over

Table 1 Parameters of our direct numerical simulations (DNS): grid resolution; mean velocity $\mathbf{U}_0$; kinematic viscosity ν; Reynolds number Re $= u_{rms}L/\nu$; and $k_{max}\eta$, where $k_{max} = N/2$ is the maximum wavenumber, and η is the Kolmogorov length

Grid	$\mathbf{U}_0$	ν	Re	$k_{max}\eta$
512^3	0	10^{-3}	5.7×10^3	2.5
512^3	$10\hat{z}$	10^{-3}	5.7×10^3	2.5
1024^3	0	4×10^{-4}	1.3×10^4	2.5

Fig. 1 For $\mathbf{U}_0 = 0$ and $\mathbf{U}_0 = 10\hat{z}$, **a** plots of total energy of the velocity fluctuation vs. t (in units of eddy turnover time). **b** Plots of the normalized kinetic energy spectrum $E(k)k^{5/3}$ vs. k. Here $E(t)$ and $E(k)$ are identical for $\mathbf{U}_0 = 0$ and $\mathbf{U}_0 = 10\hat{z}$ due to the Galilean invariance of the fluid equations
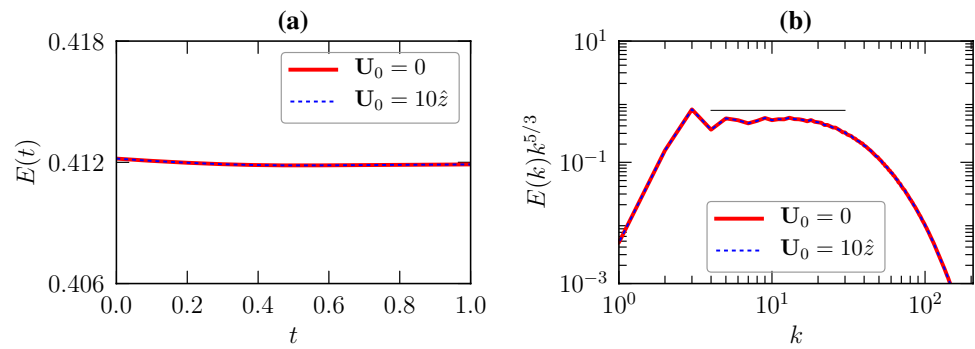
Fig. 2 For $\mathbf{U}_0 = 0$ and $k = 10, 12, 15, 20, 22$ (inertial range wavenumbers), **a** plots of the absolute value of normalised correlation function, $|R(\mathbf{k}, \tau)|$ vs. $\tau' = \tau/\tau_c$. It decays exponentially in time as in Eq. (21). **b** Plots of $|R(\mathbf{k}, \tau)| \exp(\tau/\tau_c)$ vs. τ', which is approximately flat
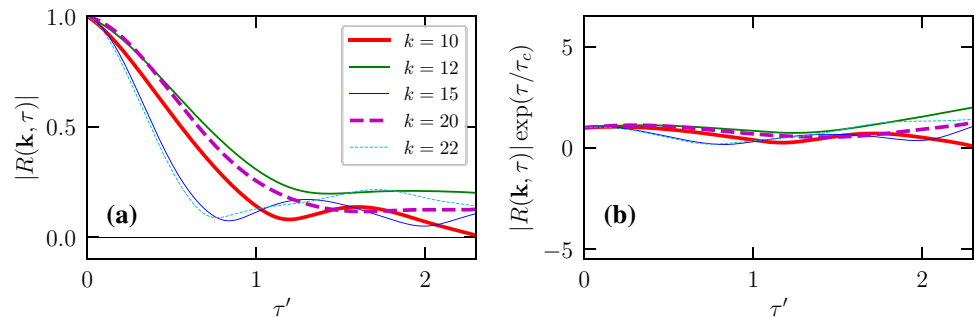
12,500 data points collected over 1.3 eddy turnover time. We observe that $R(\mathbf{k}, \tau)$ is complex, thus providing clues for the sweeping effect in the flow. In Fig. 2a we plot $|R(\mathbf{k}, \tau)|$ that decays exponentially with time with an approximate time scale of $\tau_c(k)$ given by Eq. (14). For validation of this conjecture, in Fig. 2b we plot $|R(\mathbf{k}, \tau)| \exp(\tau/\tau_c)$ which are approximate flat curves for all k's.

We compute $\tau_c(k)$ from the slope of $|R(\mathbf{k}, \tau)|$ in a semiology plot for a range of k's. A regression analysis of the data yields

$$\tau_c(k) \sim k^{-0.62 \pm 0.13}, \tag{24}$$

for k ranging from 6 to 25. The slope of -0.62 is consistent with the predicted $-2/3$ slope of Eq. (14). We exhibit the plot in Fig. 3 that exhibits some scatter, which is possibly due to the random velocity field as postulated in the sweeping effect. This observation is contrary to that of Sanada and Shanmugasundaram (1992) who argued that $\tau_c \sim k^{-1}$ based on Kraichnan (1964)'s sweeping effect arguments according to which $\tau_c \sim 1/(k\tilde{U}_0)$.

In Fig. 4 we plot $\Re[R(\mathbf{k}, \tau)]$, $\Im[R(\mathbf{k}, \tau)]$, and the phase of $R(\mathbf{k}, \tau)$, which is defined as

$$\Phi(k, \tau) = \tan^{-1} \frac{\Im[R(\mathbf{k}, \tau)]}{\Re[R(\mathbf{k}, \tau)]}. \tag{25}$$

The phase $\Phi(k, \tau)$ varies linearly till $\tau_2 \approx 0.6\tau_c$, which is the duration for the constancy of $\tilde{U}_0$. We can estimate $\tilde{U}_0$ from the phase using Eq. (21) with $|c| = 1$ (which is an
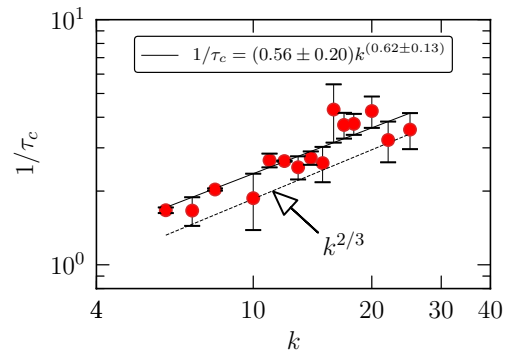

Fig. 3 Plot of τ_c^{-1} vs. k. We observe that $\tau_c^{-1} \sim k^{0.62 \pm 0.13}$. The exponent being closer to 2/3 indicates that Eq. (14) provides a fair description of the decaying time scale

assumption). From Fig. 4 we deduce the following properties for $\Phi(k, \tau)$:

1. The phase $\Phi(k, \tau)$ increases linearly with time till $\tau \approx \tau_2$, hence $\Phi(k, \tau) \propto \tau$ till $\tau \approx \tau_2$.
2. In Fig. 4, the slopes of the $\Phi(k, \tau)$ for various k's are different, hence $\Phi(k, \tau) \neq D\tau$ with a constant D for all k's. Therefore, we can easily conclude that the Fourier modes are not advected by a constant mean velocity field, say $\mathbf{U}_0$.
3. The slopes of $\Phi(k, \tau)$ come with both positive and negative signs, thus confirming random sweeping effect.

Fig. 4 For $\mathbf{U}_0 = 0$ and $k = 10, 12, 15, 20, 22$ (inertial range wavenumbers), plots of the **a** $\Re[R(\mathbf{k}, \tau)]$, **b** $\Im[R(\mathbf{k}, \tau)]$, and **c**, **d** $\Phi(\mathbf{k}, \tau)$, where $R(\mathbf{k}, \tau)$ is the normalized correlation function. Subfigure **d** is a zoomed view of **c** for $\tau' = 0 : 0.6$. The real part exhibits decaying oscillations, while the imaginary part shows oscillations, consistent with Eq. (21). The phases for various $\mathbf{k}$'s exhibit monotonic increase with time till $\tau' = \tau_2 = 0.6$ due to $\tilde{\mathbf{U}}_0$, thus demonstrating the sweeping effect
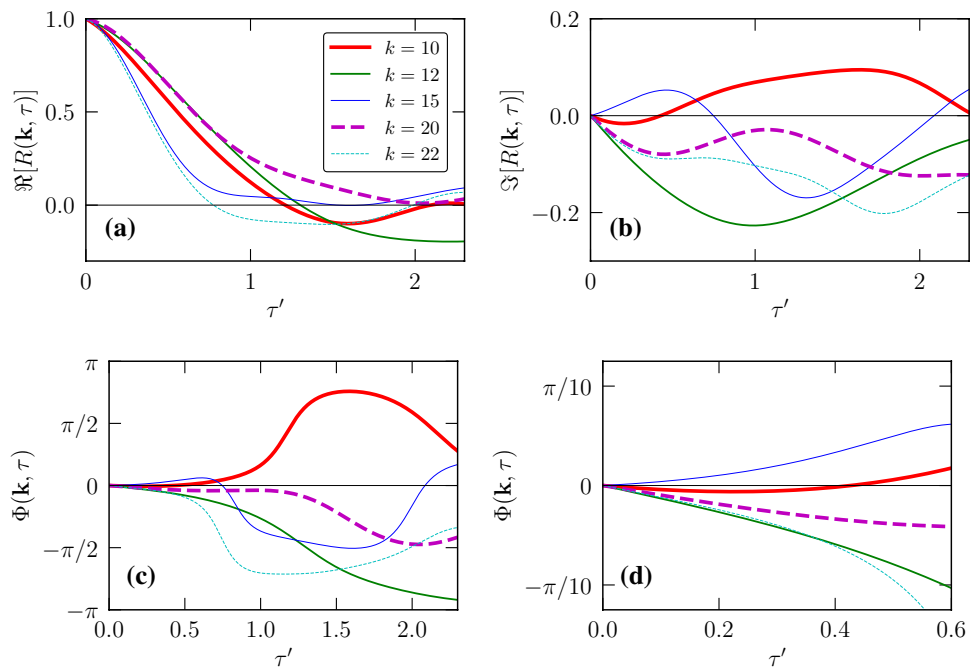
Thus, the nonzero phase $\Phi(k, \tau)$ provides evidence for the sweeping effect. In addition, the real and imaginary parts of $R(\mathbf{k}, \tau)$ contain the effects of both magnitude and phases, hence they show damped oscillations.

Hence the numerical correlation functions are consistent with Eq. (21), thus providing a numerical demonstration of the sweeping effect proposed by Kraichnan (1964). Physically, a Fourier mode $\mathbf{u}(\mathbf{k})$ is being advected by the random mean velocity field, $\tilde{U}_0(\mathbf{k})$. The random velocity changes its direction and magnitude in around an eddy turnover time. We observe that the phases are linear in τ only up to $\tau \approx \tau_2$. The aforementioned wavenumber-dependent mean velocity field is in the similar spirit as the advection of eddies within eddies (Davidson 2015; Pope 2000; McComb 1990; Verma 2019). It is important to note that the aforementioned time variation of $\tilde{U}_0(\mathbf{k})$ is contrary to the assumption of Kraichnan (1964) that $\tilde{U}_0(\mathbf{k})$ is constant in time. A detailed analysis of $\tilde{U}_0(\mathbf{k})$ as a function of wavenumber and angles, as well as its probability distribution, will be performed in future.

In the next section we analyse the sweeping effect in the presence of $\mathbf{U}_0$.

Sweeping Effect for $\mathbf{U}_0 \neq 0$

In the present section we compute $R(\mathbf{k}, \tau)$ for nonzero $\mathbf{U}_0$ using numerical data and compare it with Eq. (22). After that we will describe the frequency spectrum for zero and nonzero $\mathbf{U}_0$.

As argued in Section "A brief review of Green's function and correlation function in hydrodynamic turbulence", for nonzero $\mathbf{U}_0$, the normalised correlation function given by Eq. (22). Thus, the mean velocity field induces a factor of $\exp(-i\mathbf{U}_0 \cdot \mathbf{k}\tau)$ in the correlation function in comparison to Eq. (21) for $\mathbf{U}_0 = 0$. To verify the above correlation function, we perform numerical simulation of Eqs. (1, 2) with $\mathbf{U}_0 = 10\hat{z}$ and compute the correlation function $R(\mathbf{k}, \tau)$ for $\mathbf{k} = (0, 0, 10)$.

In Fig. 5, we plot the real and imaginary parts of the correlation $R(\mathbf{k}, \tau)$, as well as its magnitude and phase. As shown in the figure, $|R(\mathbf{k}, \tau)|$ for $\mathbf{U}_0 = 0$ and $10\hat{z}$ are approximately the same. However, both the real and imaginary parts of $R(\mathbf{k}, \tau)$ exhibit damped oscillations with a frequency of $\omega = k_z|\mathbf{U}_0|$ and a decay time scale of $1/(\nu(k)k^2)$. The oscillations are due to the $\exp(-i\mathbf{U}_0 \cdot \mathbf{k}\tau)$ term. Note that the damping time scales $\tau_c(k)$ are independent of $\mathbf{U}_0$, which is verified by the plot of Fig. 5a, b in which the envelops of $|R(\mathbf{k}, \tau)|$ and $\Re[R(\mathbf{k}, \tau)]$ match with the corresponding plots for $\mathbf{U}_0 = 0$ (shown as red lines).

The correlation function also contains signatures of the random sweeping effect for $\mathbf{U}_0 = 10\hat{z}$. In Fig. 5d, we plot the phase Φ of $R(\mathbf{k}, \tau)$, which is quite close to $U_0 k\tau$. However, $\Phi - U_0 k\tau$ is nonzero, which is evident from its magnified plot in Fig. 5d. This deviation is due to the random sweeping effect by random mean field $\tilde{U}_0$. Thus, the small-scale fluctuations are swept by $\mathbf{U}_0 = 10\hat{z}$ and by large-scale random velocity $\tilde{U}_0(k)$. Thus, sweeping effect, though overshadowed by U_0, is present for nonzero U_0 as well.

In summary, for the normalised correlation function, the absolute value $|R(\mathbf{k}, \tau)|$ falls exponentially with a decay time scale of τ_c, while the phase $\Phi(\mathbf{k}, \tau) \propto \mathbf{U}_0 \cdot \mathbf{k} + c\tilde{U}_0 k$ that contains contributions from the mean velocity and the

Fig. 5 For $\mathbf{U}_0 = 10$ and $\mathbf{k} = (0, 0, 10)$ in the inertial range, plots of the normalised correlation function $R(\mathbf{k}, \tau)$ vs. τ: **a** $\Re[R(\mathbf{k}, \tau)]$, **b** $|R(\mathbf{k}, \tau)|$, **c** $\Im[R(\mathbf{k}, \tau)]$, and **d** $\Phi(\mathbf{k}, \tau)$. The real and imaginary parts exhibit damped oscillation with the frequency of $|\mathbf{U}_0|k$ and damping time of $1/(\nu(k)k^2)$. $|R(\mathbf{k}, \tau)|$ for $\mathbf{U}_0 = 0, 10\hat{z}$ are identical, thus showing that the decay time scales for the two cases are the same; also, $|R(\mathbf{k}, \tau)|$ provides envelop to the real part. The phase of $R(\mathbf{k}, \tau)$ varies as $\Phi(\mathbf{k}, \tau) = |\mathbf{U}_0|k_z\tau + \delta$, where δ arises due to the sweeping by the random large-scale flow structures. The dashed black and blue lines represent $|\mathbf{U}_0|k_z\tau$ and 70δ (amplified by a factor for visualisation) respectively
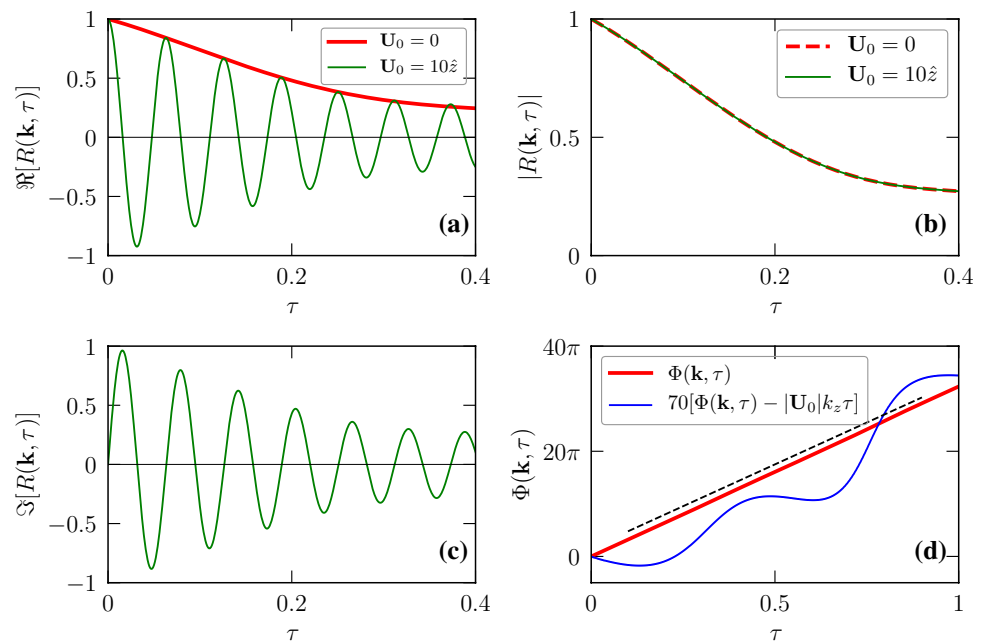
sweeping effect. Note that $|R(\mathbf{k}, \tau)|$ is independent of U_0, but the real and imaginary parts of $R(\mathbf{k}, \tau)$ contain the effects of both magnitude and phase; hence they exhibit damped oscillations.

Taylor's Frozen-in Hypothesis for $\mathbf{U}_0 \neq 0$, and Frequency Spectrum

We can use the spectral correlation function of Eq. (22) to compute the following spatio-temporal correlation (Wilczek and Narita 2012):

$$
\begin{aligned}
C(\mathbf{r}, \tau) &\sim \int d\mathbf{k}\, C(\mathbf{k}) \exp(-\nu(k)k^2\tau - i\mathbf{U_0} \cdot \mathbf{k}\tau)\langle \exp(-ick\tilde{U}_0(k)\tau)\rangle \exp(i\mathbf{k} \cdot \mathbf{r}) \\
&= \int d\mathbf{k}\, C(\mathbf{k}) \exp(-\tau/\tau_c - i\mathbf{U_0} \cdot \mathbf{k}\tau) \exp(-k^2[\tilde{U}_0(k)]^2\tau^2) \exp(i\mathbf{k} \cdot \mathbf{r}).
\end{aligned}
\tag{26}
$$

We obtain temporal correlation $C(\tau)$ measured at the same location by setting $\mathbf{r} = 0$. Fourier transform of $C(\tau)$ yields the frequency spectrum $E(f)$, which is often measured in experiments. Researchers have exploited the above hypothesis to measure turbulence spectrum in many fluid and plasma experiments, for example in wind tunnels (Tennekes and Lumley 1972), and in the solar wind using extraterrestrial spacecrafts (Matthaeus and Goldstein 1982).

In "Appendix 2: Computation of spatio-temporal correlations and frequency spectra of turbulent flow", $C(\tau)$ has been computed for the following limiting cases:

1. For nonzero $\mathbf{U}_0$ with $\mathbf{U}_0 \cdot \mathbf{k} \gg \nu(k)k^2$ and $\mathbf{U}_0 \cdot \mathbf{k} \gg k\tilde{U}_0(k)$: in this case,

$$
C(\tau) \sim (\epsilon U_0 \tau)^{2/3},
\tag{27}
$$

where ϵ is the dissipation rate that equals the energy flux. The above $C(\tau)$ yields the following frequency spectrum:

$$
E(f) \sim (\epsilon U_0)^{2/3} f^{-5/3},
\tag{28}
$$

which is the prediction of Taylor's frozen-in turbulence hypothesis. In fact, this idea is often used to test Kolmogorov's spectrum in turbulence experiments (Tennekes and Lumley 1972). Recently, Kumar and Verma (2018) and Verma (2018) invoked this scheme to deduce the energy spectrum for Rayleigh–Bénard convection in a cube when the large-scale circulation remains steady. The above spectrum also follows from Eq. (23) that yields the dominant frequency as $\omega = iU_0k_z$ for this case. See "Appendix 2: Computation of spatio-temporal correlations and frequency spectra of turbulent flow" for details. In Fig. 6a we plot $E(f)$ computed using the time series of randomly distributed 50 probes for $\mathbf{U}_0 = 10\hat{z}$ simulation. To compute the frequency spectrum $E(f)$,
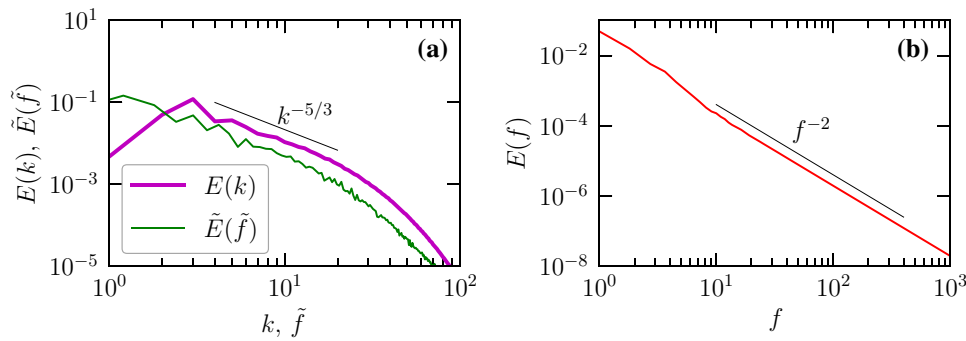
Fig. 6 a For $\mathbf{U}_0 = 10\hat{z}$, plots of the wavenumber spectrum $E(k)$ and the scaled frequency spectrum $E(f)$ for the velocity time series measured by real-space probes. The plot is averaged over 50 real-space probes located at random locations. Here $\tilde{f} = f(2\pi)/U_0$ and $\tilde{E}(\tilde{f}) = E(f)U_0/(2\pi)$. $E(f) \sim f^{-5/3}$, consistent with Taylor's frozen-in turbulence hypothesis. **b** For $\mathbf{U}_0 = 0$, $E(f) \sim f^{-2}$, consistent with the sweeping effect

we record the velocity field at the 50 real space probes. For the frequency spectrum computation, we run our simulation for a single eddy turnover time with a constant $\Delta t = 3 \times 10^{-5}$, which helps us compute the Fourier transform of the real space data using equispaced FFT. We sampled the real space data every 33 time step.

2. For $\mathbf{U}_0 = 0$: In this case,

$$C(\tau) \sim \epsilon \tau \qquad (29)$$

that yields the following frequency spectrum:

$$E(f) \sim \epsilon f^{-2}. \qquad (30)$$

As shown in the "Appendix 2: Computation of spatio-temporal correlations and frequency spectra of turbulent flow", the above spectrum is a result of $\exp(-k^2[\tilde{U}_0(k)]^2\tau^2)$ (sweeping effect) and $\exp(-\tau/\tau_c)$ (damping term). The above spectrum can be derived using the dominant frequency relation $\omega = \nu(k)k^2$. See "Appendix 2: Computation of spatio-temporal correlations and frequency spectra of turbulent flow" for details. Also see Fig. 6b for an illustration of $E(f)$ computed using the time series of randomly distributed 50 probes for the $\mathbf{U}_0 = 0$ simulation.

We can also derive Taylor's frozen-in hypothesis in the following manner. For $\mathbf{U}_0 = 0$ and setting $\tau = 0$, Eq. (26) yields equal-time correlation as

$$C(\mathbf{r}, \tau = 0) = \int d\mathbf{k} C(\mathbf{k}) \exp(i\mathbf{k} \cdot \mathbf{r}). \qquad (31)$$

On the other hand, if we set $\mathbf{r} = 0$ and assume that $\mathbf{U}_0 \cdot \mathbf{k} \gg \nu(k)k^2$ and $\mathbf{U}_0 \cdot \mathbf{k} \gg k\tilde{U}_0(k)$, then Eq. (26) yields

$$C(\mathbf{r} = 0, \tau) = \int d\mathbf{k} C(\mathbf{k}) \exp(-i\mathbf{U}_0 \cdot \mathbf{k}\tau), \qquad (32)$$

which has a very similar structure as Eq. (31) with $\mathbf{r}$ replaced by $-\mathbf{U}_0\tau$. Hence

$$C(\mathbf{r} = 0, \tau) = C(\mathbf{r}, \tau = 0) \quad \text{with } \mathbf{r} = -\mathbf{U}_0\tau. \qquad (33)$$

That is, equal-time spatial correlation (for $\mathbf{U}_0 = 0$) is related to the equal-space temporal correlation for nonzero $\mathbf{U}_0$. This is the essence of Taylor's frozen-in hypothesis. We illustrate the physical interpretation of the above result in Fig. 7. It is important to note that Eq. (33) is valid for any kind of flow, turbulent or viscous.

For steady, homogeneous, and isotropic turbulence, and for r in the inertial range, (Kolmogorov 1941a, b) derived that

$$C(r) = c_1 - c_2(\epsilon r)^{2/3}, \qquad (34)$$
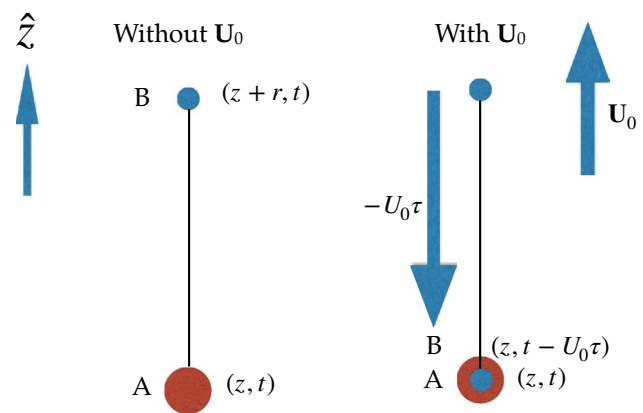
Fig. 7 In the left figure, A and B represent respectively the velocity measurements at locations z and $z + r$ and at times t (same time) when $\mathbf{U}_0 = 0$. In the right figure, the measurements are performed at the same place ($z = 0$), but at different times, t and $t - U_0\tau$. Here $\mathbf{U}_0$ is along the z axis. According to Taylor's hypothesis, the velocity correlations of the two figures are the same

where c_1 and c_2 are constants. The above relation and inverse transform of Eq. (31) yields $C(\mathbf{k}) \sim \epsilon^{2/3} k^{-11/3}$ that leads to $E(k) \sim k^{-5/3}$, which is Kolmogorov's spectrum. Note that $\tilde{U}_0(k)$ or the sweeping effect does not affect the $k^{-5/3}$ spectrum. Substitution of the above $C(\mathbf{k})$ in Eq. (32) yields

$$C(\tau) = c_3 (\epsilon U_0 \tau)^{2/3}, \tag{35}$$

where c_3 is a constant. Fourier transform of the above equation yields Eq. (28). This is a alternative derivation of Taylor's frozen-in hypothesis.

Tennekes and Lumley (1972) termed the correlation associated with $f^{-5/3}$ spectrum as Eulerian space-time correlation due to its connection with the mean flow $\mathbf{U}_0$ that advects the flow, reminiscent of Eulerian picture. The frequency spectrum f^{-2} is associated with the fluctuating "mean velocity", hence Tennekes and Lumley (1972) called the associated correlation as Lagrangian space-time correlation, possibly relating the sweeping effect with random scattering of particles. Note, however, that we derived both these spectra in Eulerian hydrodynamics framework.

He et al. (2010), and He and Tong (2011) combined the sweeping effect with Taylor's frozen-in turbulence hypothesis in a framework called elliptic approximation. Due to the sweeping effect, the isocontour lines of the equal-time correlation function measured at two different locations separated by $\mathbf{r}_E$ is the following elliptical function (deviates from a straight line, a prediction of Taylor's hypothesis):

$$r_E^2 = r_{Ez}^2 + |\mathbf{r}_{E\perp}|^2 = [r - (U_0 + \tilde{U}_{0z})\tau]^2 + [|\tilde{\mathbf{U}}_{0\perp}|\tau]^2. \tag{36}$$

In the above expression, $\tilde{U}_{0z}$ and $\tilde{\mathbf{U}}_{0\perp}$ are the parallel and perpendicular components of the random velocity field along and perpendicular to $\mathbf{U}_0$. Refer to He et al. (2010) and He and Tong (2011), and Appendix "Elliptic approximation" for further details. Thus, the sweeping effect, Taylor's frozen-in turbulence hypothesis, and space-time correlation functions are related to each other.

We conclude in the next section.

Discussions and conclusions

Using numerical simulations, we demonstrate the presence of sweeping effect in hydrodynamic turbulence. For zero mean flow ($\mathbf{U}_0 = 0$), we compute the velocity correlation function $C(k, \tau)$ and show that its magnitude decays with time-scale $\tau_c \approx 1/(\nu(k)k^2)$, where $\nu(k)$ is the renormalised viscosity. However, the phase of the correlation function shows a linear increase with τ till approximately one eddy turnover time; this is attributed to the sweeping of the small scale fluctuations by the random mean velocity, $\tilde{\mathbf{U}}_0$, of the flow. Thus we demonstrate a clear signature of sweeping effect in hydrodynamic turbulence. Note that the phase of the

correlation function extracts the sweeping effect by random mean velocity. Our approach deviates from those of Sanada and Shanmugasundaram (1992) who only studied the absolute of correlation function and argued that $\tau_c \sim k^{-1}$, in line with the predictions of Kraichnan (1964). On the contrary, our simulations shows that $\tau_c \sim k^{-2/3}$.

For nonzero mean flow ($\mathbf{U}_0 = 10\hat{z}$), the correlation function exhibits damped oscillations with a frequency of $\omega = U_0 k$ and decay time scale of $1/(\nu(k)k^2)$; the decay time scales for $\mathbf{U}_0 = 10\hat{z}$ is same as that for $\mathbf{U}_0 = 0$. A careful examination of the phase of the correlation function also shows additional variations due to the sweeping by the random mean velocity $\tilde{\mathbf{U}}_0$ of the flow.

For the aforementioned two cases, the frequency spectra of the velocity field measured by the real-space probes are different. For $\mathbf{U}_0 = 0$, $E(f) \sim f^{-2}$, which is related to the Lagrangian space-time correlation, but for $\mathbf{U}_0 = 10\hat{z}$, $E(f) \sim f^{-5/3}$, which is the predictions of Taylor's frozen-in turbulence hypothesis. We demonstrate these spectra using their respective space-time correlation functions. Our analysis shows that Taylor's hypothesis is applicable when

$$U_0 k \gg \nu(k)k^2; \quad U_0 \gg \tilde{U}_0, \tag{37}$$

where $\tilde{U}_0$ is random mean velocity, which is responsible for the sweeping effect.

Thus, we provide a systematic demonstration of sweeping effect and Taylor's frozen-in turbulence hypothesis, and show consistency between the two contrasting phenomena. We demonstrate the above spectra using numerical simulations.

Author Contributions MKV performed theoretical formulation and calculations. AK performed numerical simulations and data analysis. AG performed the analysis for 1024^3 data. MKV and AK wrote the paper.

Appendix 1: Sweeping Effect and Renormalization in Eulerian Framework

In this section we extend iterative renormalisation group (i-RG) of McComb (1990) and Zhou (2010) to include the effects of the mean velocity field $\mathbf{U}_0$. We show that the renormalised viscosity is independent of $\mathbf{U}_0$. However, this scheme fails to capture the sweeping effect. This issue was first raised by Kraichnan (1964) in direct interaction

approximation (DIA) framework. Note that the above computations are based on Eulerian framework. Since the above RG scheme is covered in detail in many references, such as McComb (1990), Zhou (2010) and Verma (2001, (2004), here we highlight the changes induced by $\mathbf{U}_0$.

In Fourier space, the Navier–Stokes equations in the presence of $\mathbf{U}_0$ are (McComb 1990)

$$(-i\omega + i\mathbf{U}_0 \cdot \mathbf{k} + \nu k^2)u_i(\hat{k}) = -\frac{i}{2}P_{ijm}(\mathbf{k}) \int_{\hat{p}+\hat{q}=\hat{k}} d\hat{p}\left[u_j(\hat{p})u_m(\hat{q})\right] + f_i(\hat{k}),$$
(38)

$$k_i u_i(\mathbf{k}) = 0,$$
(39)

where

$$\delta\nu_{(n)}(\omega, k)k^2 = \frac{1}{d-1} \int_{\hat{p}+\hat{q}=\hat{k}} \frac{d\mathbf{p}d\omega'}{(2\pi)^{d+1}} B(k, p, q)C(\mathbf{p})$$

$$\times \frac{1}{\left[-i\omega + i\omega' + i\mathbf{U}_0 \cdot \mathbf{q} + \nu_{(n)}(q)q^2\right]\left[-i\omega' + i\mathbf{U}_0 \cdot \mathbf{p} + \nu_{(n)}(p)p^2\right]}$$

$$= \frac{1}{d-1} \int_{\mathbf{p}+\mathbf{q}=\mathbf{k}}^{\Delta} \frac{d\mathbf{p}}{(2\pi)^d} \frac{B(k, p, q)C(\mathbf{p})}{\left[-i(\omega - \mathbf{U}_0 \cdot \mathbf{k}) + \nu_{(n)}(p)p^2 + \nu_{(n)}(q)q^2\right]}$$

$$= \frac{1}{d-1} \int_{\mathbf{p}+\mathbf{q}=\mathbf{k}}^{\Delta} \frac{d\mathbf{p}}{(2\pi)^d} \frac{B(k, p, q)C(\mathbf{p})}{\nu_{(n)}(p)p^2 + \nu_{(n)}(q)q^2}.$$
(46)

$$P_{ijm}(\mathbf{k}) = k_j P_{im}(\mathbf{k}) + k_m P_{ij}(\mathbf{k}),$$

$$\hat{k} = (\omega, \mathbf{k}), \hat{p} = (\omega', \mathbf{p}), \text{ and } \hat{q} = (\omega'', \mathbf{q}); \quad \hat{k} = \hat{p} + \hat{q}.$$
(40)

We compute the renormalized viscosity in the presence of a mean velocity $\mathbf{U}_0$. In the renormalization process, the wavenumber range (k_N, k_0) is divided logarithmically into N shells. The nth shell is (k_n, k_{n-1}) where $k_n = h^n k_0$ $(h < 1)$ and $k_N = h^N k_0$. In the first step, the spectral space is divided in two parts: the shell $(k_1, k_0) = k^>$, which is to be eliminated, and $(k_N, k_1) = k^<$, set of modes to be retained. The velocity modes in the $k^>$ regime are averaged. The averaging procedure enhances the viscosity, and the new viscosity is called "renormalized viscosity". The process is continued for other shells that leads to larger and larger viscosity.

In i-RG scheme, after $(n + 1)$st step, the renormalized equation appears as

$$\left[-i\omega + i\mathbf{U}_0 \cdot \mathbf{k} + (\nu_{(n)}(k) + \delta\nu_{(n)}(k))k^2\right]u_i^<(\hat{k}) =$$
$$-\frac{i}{2}P_{ijm}(\mathbf{k}) \int_{\hat{p}+\hat{q}=\hat{k}} \frac{d\mathbf{p}d\omega'}{(2\pi)^{d+1}} [u_j^<(\hat{p})u_m^<(\hat{k}-\hat{p})] + f_i^<(\hat{k})$$
(41)

with

$$\delta\nu_{(n)}(\hat{k})k^2 = \frac{1}{d-1} \int_{\hat{p}+\hat{q}=\hat{k}}^{\Delta} \frac{d\mathbf{p}d\omega'}{(2\pi)^{d+1}} [B(k, p, q)G(\hat{q})C(\hat{p})].$$
(42)

In the above expression,

$$B(k, p, q) = kp[(d-3)z + 2z^3 + (d-1)xy],$$
(43)

where d is the space dimensionality, x, y, z are the direction cosines of $\mathbf{k}, \mathbf{p}, \mathbf{q}$, and $G(\hat{q}), C(\hat{p})$ are respectively Green's and correlation functions that are defined as (McComb 1990; Zhou 2010; Verma 2004)

$$G(\hat{q}) = \frac{1}{-i\omega'' + i\mathbf{U}_0 \cdot \mathbf{q} + \nu_{(n)}(q)q^2},$$
(44)

$$C(\hat{p}) = \frac{C(\mathbf{p})}{-i\omega' + i\mathbf{U}_0 \cdot \mathbf{p} + \nu_{(n)}(p)p^2}.$$
(45)

Using $\omega = \omega' + \omega''$, we obtain

Note that $\omega - \mathbf{U}_0 \cdot \mathbf{k} = \omega_D$ is the Doppler-shifted frequency in the moving frame, where the frequency of the signal is reduced. It is analogous to the reduction of frequency of the sound wave in a moving train when the train moves away from the source. For $\mathbf{U}_0 = 0$, it is customary to assume that $\omega \to 0$ since we focus on dynamics at large time scales (McComb 1990; Zhou 2010; McComb 2014). The corresponding assumption for $\mathbf{U}_0 \neq 0$ is to set $\omega_D \to 0$ because ω_D is the effective frequency of the large scale modes in the moving frame. The approximation $\omega \to \omega_D$ essentially takes away the effect of Galilean transformation and provides inherent turbulence properties. Note that in Taylor's frozen-in turbulence hypothesis, $\omega = \mathbf{U}_0 \cdot \mathbf{k}$ that yields $\omega_D = 0$ (Tennekes and Lumley 1972).

Equation (46) indicates that the correction in viscosity, $\delta\nu_{(n)}$, is independent of $\mathbf{U}_0$. After this step, the derivation of renormalised viscosity with and without $\mathbf{U}_0$ are identical. Equation (46) however does not include any sweeping effect, which is a serious limitation of Eulerian field theory, as pointed out by Kraichnan (1964) in direct interaction approximation (DIA) framework. Kraichnan (1965) then formulated Lagrangian-history closure approximation for turbulence and showed consistency with Kolmogorov's spectrum (also see Leslie 1973). Effectively, a consistent theory needs to include a term of the form $i\tilde{\mathbf{U}}_0 \cdot \mathbf{q}$ in the denominator of Eq. (44). A procedure adopted by Verma

(1999) for "mean magnetic field" renormalisation in magnetohydrodynamic turbulence may come out to be handy for such computations, which may be attempted in future.

Appendix 2: Computation of Spatio-Temporal Correlations and Frequency Spectra of Turbulent Flow

Using the normalized correlation function of Eq. (22), we derive the following spatio-temporal correlation function:

$$C(\mathbf{r}, \tau) = \int d\mathbf{k} C(\mathbf{k}) \exp(-\nu(k)k^2\tau - i\mathbf{U_0} \cdot \mathbf{k}\tau) \exp(-i\mathbf{k} \cdot \tilde{\mathbf{U}}_0(\mathbf{k})\tau) \exp(i\mathbf{k} \cdot \mathbf{r}). \tag{47}$$

We time average $\tilde{U}_0$ over random ensemble (Kraichnan 1964; Wilczek and Narita 2012) that yields

$$C(\mathbf{r}, \tau) = \int d\mathbf{k} C(\mathbf{k}) \exp(-\nu(k)k^2\tau - i\mathbf{U_0} \cdot \mathbf{k}\tau)\langle \exp(-ick\tilde{U}_0(k)\tau)\rangle \exp(i\mathbf{k} \cdot \mathbf{r})$$
$$= \int d\mathbf{k} C(\mathbf{k}) \exp(-\tau/\tau_c - i\mathbf{U_0} \cdot \mathbf{k}\tau) \exp(-k^2[\tilde{U}_0(k)]^2\tau^2) \exp(i\mathbf{k} \cdot \mathbf{r}). \tag{48}$$

In addition, we set $\mathbf{r} = 0$ to compute the temporal correlation at a single point.

In the above integral, following Pope (2000), we replace the isotropic and homogeneous $C(\mathbf{k})$ with

$$C(\mathbf{k}) = \frac{E(k)}{4\pi k^2} = \frac{f_L(kL)f_\eta(k\eta)K_{Ko}\epsilon^{2/3}k^{-5/3}}{4\pi k^2}, \tag{49}$$

where ϵ is the energy dissipation rate, which is same as the energy flux, and

$$f_L(kL) = \left(\frac{kL}{[(kL)^2 + c_L]^{1/2}}\right)^{5/3 + p_0}, \tag{50}$$

$$f_\eta(k\eta) = \exp\left[-\beta\left\{[(k\eta)^4 + c_\eta^4]^{1/4} - c_\eta\right\}\right], \tag{51}$$

with c_L, c_η, p_0, β as constants, and L as the large length scale of the system. We also substitute $\tau_c(k) = 1/(\nu(k)k^2) = \epsilon^{-1/3}k^{-2/3}$ and $\tilde{U}_0(k) = \epsilon^{1/3}k^{-1/3}$ (from dimensional analysis). We ignore the coefficients in front of these quantities for brevity. After the above substitutions, we obtain

$$C(\tau) = K_{Ko}\epsilon^{2/3} \int dk k^{-5/3} f_L(kL)f_\eta(k\eta) \exp(-i\mathbf{U_0} \cdot \mathbf{k}\tau)\times$$
$$\exp(-\epsilon^{1/3}k^{2/3}\tau) \exp(-\epsilon^{2/3}k^{4/3}\tau^2). \tag{52}$$

The above form of $C(\tau)$ is valid for any $\mathbf{U_0}$. The above integral is too complex, hence we perform asymptotic analysis in two limiting cases that are described below.

For $\mathbf{U_0} \cdot \mathbf{k} \gg \nu(k)k^2$ and $\mathbf{U_0} \cdot \mathbf{k} \gg k\tilde{U}_0(k)$

For this case U_0 dominates other velocity scales, hence we take $\tau \sim 1/(U_0k)$ as the dominant time scale. For simplification, we make a change of variable, $\tilde{k} = U_0k\tau$. In addition, we choose the z axis to be along the direction of $\mathbf{U}_0$. Under these simplifications, the integral becomes

$$C(\tau) \approx K_{Ko}(\epsilon U_0\tau)^{2/3} \int d\tilde{k}\tilde{k}^{-5/3}f_L(\tilde{k}(L/U_0\tau))f_\eta(\tilde{k}(\eta/U_0\tau)\frac{\sin(U_0k\tau)}{U_0k\tau}$$
$$\times \exp[-\tilde{k}^{2/3}(U/U_0)^{2/3}(\tau/T)^{1/3} - \tilde{k}^{4/3}(U/U_0)^{4/3}(\tau/T)^{2/3}]. \tag{53}$$

We focus on τ in the inertial range, hence $L/U_0\tau \gg 1$ and $\eta/U_0\tau \ll 1$, consequently, $f_L(\tilde{k}(L/U_0\tau)) \approx 1$, and $f_\eta(\tilde{k}(\eta/U_0\tau) \approx 1$. Therefore,

$$C(\tau) \approx K_{Ko}(\epsilon U_0\tau)^{2/3} \int d\tilde{k}\tilde{k}^{-5/3}\frac{\sin \tilde{k}}{\tilde{k}} \exp[-\tilde{k}^{2/3}(U/U_0)^{2/3}(\tau/T)^{1/3} - \tilde{k}^{4/3}(U/U_0)^{4/3}(\tau/T)^{2/3}]$$
$$\approx BK_{Ko}(\epsilon U_0\tau)^{2/3}, \tag{54}$$

where B is the value of the nondimensional integral. The Fourier transform of the above $C(\tau)$ yields the following frequency spectrum:

$$E(f) \approx \int C(\tau) \exp(i2\pi f\tau)d\tau = \int BK_{Ko}(\epsilon U_0\tau)^{2/3} \exp(i2\pi f\tau)d\tau$$
$$\sim (\epsilon U_0)^{2/3}f^{-5/3}. \tag{55}$$

The above frequency spectrum is the prediction of Taylor's frozen-in turbulence hypothesis.
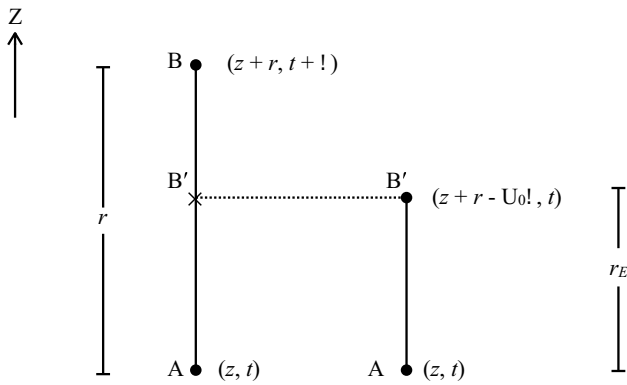
Fig. 8 A and B represent respectively the velocity measurements at locations z and $z + r$ and at times t and $t + \tau$. The fluid element at B would be at B′ at time t, thus A and B′ would represent equal-time measurements. Note that $r_E = r - U_0\tau$

For $U_0 = 0$

We set $U_0 = 0$ in Eq. (52). In the resulting equation, both the remaining exponential terms (the damping and sweeping effect terms) have the following time scale:

$$\tau(k) \sim 1/(ku_k) \sim \epsilon^{-1/3}k^{-2/3}. \qquad (56)$$

Hence, for computing the integral $C(\tau)$, we make a change of variable:

$$k = \tilde{k}\epsilon^{-1/2}\tau^{-3/2} \qquad (57)$$

that transforms the integral to

$$C(\tau) \approx K_{\mathrm{Ko}}\epsilon\tau \int d\tilde{k}\tilde{k}^{-5/3} f_L(\tilde{k}(L/U\tau)^{3/2}) f_\eta(\tilde{k}(\tau_d/\tau)^{3/2}) \exp(-\tilde{k}^{2/3} - \tilde{k}^{4/3}), \qquad (58)$$

where U is the large-scale velocity, and τ_d is the dissipative time scale. We focus on τ in the inertial range, hence $L/U\tau \gg 1$ and $\tau_d/\tau \ll 1$. Therefore, using Eqs. (50), (51), we deduce that $f_L(\tilde{k}(L/U\tau)^{3/2}) \approx 1$ and $f_\eta(\tilde{k}(\tau_d/\tau)^{3/2}) \approx 1$. Therefore,

$$C(\tau) \approx K_{\mathrm{Ko}}\epsilon\tau \int d\tilde{k}\tilde{k}^{-5/3} \exp(-\tilde{k}^{2/3} - \tilde{k}^{4/3}) \approx A K_{\mathrm{Ko}}\epsilon\tau, \qquad (59)$$

where A is the value of the integral of Eq. (59). The Fourier transform of $C(\tau)$ yields the following frequency spectrum:

$$C(f) = \int C(\tau) \exp(i2\pi f\tau)\mathrm{d}\tau = A K_{\mathrm{Ko}}\epsilon \int \tau \exp(i2\pi f\tau)\mathrm{d}\tau \sim \epsilon f^{-2}. \qquad (60)$$

Thus, the damping and sweeping terms yield frequency spectrum $E(f) \sim f^{-2}$.

We could also derive the above frequency spectra using scaling arguments Landau and Lifshitz (1987). From Eq. (23), we obtain the dominant frequency as

$$\omega = \mathbf{U}_0 \cdot \mathbf{k} + ck\tilde{U}_0(k) - i\nu(k)k^2. \qquad (61)$$

When $\mathbf{U}_0 \cdot \mathbf{k} \gg \nu(k)k^2$ and $\mathbf{U}_0 \cdot \mathbf{k} \gg k\tilde{U}_0(k)$, we obtain $\omega = U_0 k_z$. Therefore, using the formula for one-dimensional spectrum $E(k) = K_{\mathrm{Ko}}\epsilon^{2/3}k^{-5/3}$, and $\omega = 2\pi f$, we obtain

$$E(f) = E(k)\frac{\mathrm{d}k}{\mathrm{d}f} \sim (\epsilon U_0)^{2/3} f^{-5/3}. \qquad (62)$$

On the contrary, when $\mathbf{U}_0 \cdot \mathbf{k} \ll \nu(k)k^2$ (for zero or small U_0), we obtain $\omega \approx \nu(k)k^2 = \nu_* \sqrt{K_{\mathrm{Ko}}}\epsilon^{1/3}k^{2/3}$ and hence,

$$E(f) = E(k)\frac{\mathrm{d}k}{\mathrm{d}f} \sim \epsilon f^{-2}, \qquad (63)$$

consistent with the formulas derived earlier.

The spectral exponent (-2) for Burgers equation matches the above exponent for the frequency spectrum (for the $U_0 = 0$ case). However, there are important differences between Burgers turbulence and hydrodynamic turbulence. Burgers turbulence exhibits k^{-2} spectrum in wavenumber space (e.g. see Verma 2000), but hydrodynamic turbulence for $U_0 = 0$ case shows f^{-2} spectrum in frequency space. The k^{-2} spectrum in the Burgers turbulence is related to shocks, but f^{-2} spectrum for hydrodynamics has no connection to shocks.

Elliptic Approximation

In Section "Taylor's Frozen-in hypothesis for $\mathbf{U}_0 \neq 0$, and frequency spectrum" we showed that the equal-time velocity correlation for $\mathbf{U}_0 = 0$ matches with unequal-space temporal correlation for nonzero $\mathbf{U}_0$ (see Eq. (33)). Elliptic approximation combines the Taylor's frozen-in hypothesis with the sweeping effect. This task was performed by He et al. (2010) and He and Tong (2011). Here, we reproduce their arguments using Eq. (47).

We consider a fluid flow with a mean velocity of $\mathbf{U}_0$ along the z axis. We focus on the vertical velocities measured at two points z and $z + r$, but at times t and $t + \tau$ (see Fig. 8 for an illustration). For the same, the space-time correlation derived using Eq. (47) is

$$C(r, \tau) = \int d\mathbf{k}C(\mathbf{k}) \exp(-\nu(k)k^2\tau) \exp\left\{[r - i(U_0 + \tilde{U}_{0z})\tau]ik_z - i\tilde{\mathbf{U}}_{0\perp} \cdot \mathbf{k}_\perp\tau\right\}. \qquad (64)$$

Now suppose that

$$r \approx U_0 \tau \gg \nu(k)k^2\tau, \tag{65}$$

then

$$C(r, \tau) = \int d\mathbf{k}\, C(\mathbf{k}) \exp \left\{ [r - (U_0 + \tilde{U}_{0z})\tau)]ik_z - i\tilde{\mathbf{U}}_{0\perp} \cdot \mathbf{k}_\perp \tau \right\}. \tag{66}$$

We can relate the above correlation function to an equal-time correlation function

$$C(\mathbf{r}_E, 0) = \exp[ir_{Ez}k_z + i\mathbf{r}_{E\perp} \cdot \mathbf{k}_\perp] \tag{67}$$

with

$$r_{Ez} = [r - (U_0 + \tilde{U}_{0z})\tau)]; \ \mathbf{r}_{E\perp} = \tilde{\mathbf{U}}_{0\perp}\tau \tag{68}$$

or

$$r_E^2 = r_{Ez}^2 + |\mathbf{r}_{E\perp}|^2 = (r - U\tau)^2 + (V\tau)^2, \tag{69}$$

where

$$U = U_0 + \tilde{U}_{0z} \tag{70}$$

$$V = |\tilde{\mathbf{U}}_{0\perp}|. \tag{71}$$

This is the statement of elliptic approximation (He et al. 2010; He and Tong 2011). Our derivation is slightly different from those of He et al. (2010) and He and Tong (2011).

Thus, the elliptic approximation includes both, the sweeping effect and Taylor's frozen-in turbulence hypothesis. The velocities U_0 and $\tilde{U}_0$ yield the Eulerian and Lagrangian space-time correlations respectively, and they are related to the sweeping effect and Taylor's hypothesis respectively. It is easy to see that the conventional Taylor's hypothesis is applicable when $U_0 \gg \tilde{U}_0$ and it yields $f^{-5/3}$ spectrum, for which the physical interpretation is as follows. The velocity correlation for the velocity measurements at A and B of Fig. 8, $C(r, \tau) = \langle \mathbf{u}(z, t)\mathbf{u}(z + r, t + \tau) \rangle$, is same as those measured at A and B$'$ at the same time t, $C(r_E, 0) = \langle \mathbf{u}(z, t)\mathbf{u}(z + r - U_0\tau, t) \rangle$. This is because the fluid element at B$'$ at time t reaches B at time $t + \tau$.

References

Belinicher VI, L'vov VS (1987) A scale invariant theory of fully developed hydrodynamic turbulence. JETP 66:303–313

Carati D, Ghosal S, Moin P (1995) On the representation of backscatter in dynamic localisation models. Phys Fluids 7(3):606–616

Chatterjee AG, Verma MK, Kumar A, Samtaney R, Hadri B, Khurram R (2017) Scaling of a Fast Fourier Transform and a pseudo-spectral fluid solver up to 196,608 cores. J Parallel Distrib Comput 113:77–91

Davidson PA (2015) Turbulence, 2nd edn. Oxford University Press, Oxford

De Dominicis C, Martin PC (1979) Energy spectra of certain randomly-stirred fluids. Phys Rev A 19(1):419

Drivas TD, Johnson PL, Cristian C, Wilczek M (2017) Large-scale sweeping of small-scale eddies in turbulence: a filtering approach. Phys Rev Fluids 10:104603

Frisch U (1995) Turbulence. Cambridge University Press, Cambridge

He X, Tong P (2011) Kraichnan's random sweeping hypothesis in homogeneous turbulent convection. Phys Rev E 83:037302

He X, He G, Tong P (2010) Small-scale turbulent fluctuations beyond Taylor's frozen-flow hypothesis. Phys Rev E 81(6):065303(R)

Kiyani K, McComb WD (2004) Time-ordered fluctuation–dissipation relation for incompressible isotropic turbulence. Phys Rev E 70:066303

Kolmogorov AN (1941) Dissipation of energy in locally isotropic turbulence. Dokl Acad Nauk SSSR 32(1):16–18

Kolmogorov AN (1941) The local structure of turbulence in incompressible viscous fluid for very large Reynolds numbers. Dokl Acad Nauk SSSR 30(4):301–305

Kraichnan RH (1959) The structure of isotropic turbulence at very high Reynolds numbers. J Fluid Mech 5:497–543

Kraichnan RH (1964) Kolmogorov's hypotheses and Eulerian turbulence theory. Phys Fluids 7(11):1723

Kraichnan RH (1965) Lagrangian-history closure approximation for turbulence. Phys Fluids 8(4):575–598

Kumar A, Verma MK (2018) Applicability of Taylor's hypothesis in thermally driven turbulence. R Soc Open Sci 5:172152–173015

Landau LD, Lifshitz EM (1987) Fluid mechanics. Butterworth–Heinemann, Oxford

Lesieur M (2012) Turbulence in fluids, 4th edn. Springer, Dordrecht

Leslie DC (1973) Developments in the theory of turbulence. Clarendon Press, Oxford

Matthaeus WH, Goldstein ML (1982) Measurement of the rugged invariants of magnetohydrodynamic turbulence in the solar wind. J Geophys Res 87:6011–6028

McComb WD (1990) The physics of fluid turbulence. Clarendon Press, Oxford

McComb WD (2014) Homogeneous, isotropic turbulence: phenomenology, renormalisation and statistical closures. Oxford University Press, Oxford

Novikov EA (1965) Functionals and the random force method in turbulence. JETP 20:1290

Pope SB (2000) Turbulent flows. Cambridge University Press, Cambridge

Sanada T, Shanmugasundaram V (1992) Random sweeping effect in isotropic numerical turbulence. Phys Fluids A 4(6):1245

Taylor GI (1938) The spectrum of turbulence. Proc R Soc A 164(9):476–490

Tennekes H, Lumley JL (1972) A first course in turbulence. MIT Press, Cambridge

Verma MK (1999) Mean magnetic field renormalisation and Kolmogorov's energy spectrum in magnetohydrodynamic turbulence. Phys Plasmas 6(5):1455–1460

Verma MK (2000) Intermittency exponents and energy spectrum of the Burgers and KPZ equations with correlated noise. Phys A 8:359–388

Verma MK (2001) Field theoretic calculation of renormalised-viscosity, renormalised-resistivity, and energy fluxes of magnetohydrodynamic turbulence. Phys Plasmas 64:26305

Verma MK (2004) Statistical theory of magnetohydrodynamic turbulence: recent results. Phys Rep 401(5):229–380

Verma MK (2018) Physics of buoyant flows: from instabilities to turbulence. World Scientific, Singapore

Verma MK (2019) Energy transfers in fluid flows: multiscale and spectral perspectives. Cambridge University Press, Cambridge

Verma MK, Chatterjee A, Reddy KS, Yadav RK, Paul S, Chandra M, Samtaney R (2013) Benchmarking and scaling studies of pseudospectral code Tarang for turbulence simulations. Pramana J Phys 81:617–629

Wilczek M, Narita Y (2012) Wave-number-frequency spectrum for turbulence from a random sweeping hypothesis with mean flow. Phys Rev E 86(6):066308

Yakhot V, Orszag SA (1986) Renormalization group analysis of turbulence. I. Basic Theory J Sci Comput 1(1):3–51

Zhou Y (2010) Renormalization group theory for fluid and plasma turbulence. Phys Rep 488(1):1–49